JOURNAL OF SYNCHROTRON RADIATION
ISSN 1600-5775

BL-02: a versatile X-ray scattering and diffraction beamline for engineering applications at Indus-2 synchrotron source

Pooja Gupta,[a,b]* P. N. Rao,[a] M. K. Swami,[a] A. Bhakar,[a,b] Sohan Lal,[a] S. R. Garg,[a] C. K. Garg,[a] P. K. Gauttam,[a] S. R. Kane,[a] V. K. Raghuwanshi[a] and S. K. Rai[a]*

[a]Synchrotrons Utilisation Section, Raja Ramanna Centre for Advanced Technology, PO RRCAT, Indore, Madhya Pradesh 452013, India, and [b]Homi Bhabha National Institute, Training School Complex, Anushaktinagar, Mumbai, Maharashtra 400094, India. *Correspondence e-mail: drgpooja@gmail.com, sanjayrai@rrcat.gov.in

Received 15 March 2021
Accepted 3 May 2021

Edited by K. Kvashnina, ESRF – The European Synchrotron, France

Keywords: synchrotron radiation; ADXRD; EDXRD; residual stress; XRR.

A hard X-ray engineering applications beamline (BL-02) was commissioned recently and started operation in March 2019 at the Indian synchrotron source, Indus-2. This bending-magnet-based beamline is capable of operating in various beam modes, *viz.* white, pink and monochromatic beam. The beamline utilizes the X-ray diffraction technique in energy-dispersive and angle-dispersive modes to carry out experiments mainly focused on engineering problems, *viz.* stress measurement, texture measurement and determination of elastic constants in a variety of bulk as well as thin-film samples. An open-cradle six-circle diffractometer with ∼12 kg load capacity allows accommodation of a wide variety of engineering samples and qualifies the beamline as a unique facility at Indus-2. The high-resolution mode of this beamline is suitably designed so as to carry out line profile analysis for characterization of micro- and nano-structures. In the present article the beamline is described starting from the beamline design, layout, optics involved, various operational modes and experimental stations. Experiments executed to validate the beamline design parameters and to demonstrate the capabilities of the beamline are also described. The future facilities to be incorporated to enhance the capabilities of the beamline are also discussed.

1. Introduction

Residual stresses are commonly found in bulk and thin films as a consequence of the fabrication process. Also, stresses are modified during service depending on the environment and loading conditions experienced by the components. The presence of residual stresses and texture can significantly affect the performance of the components. True measurement of residual stresses and texture is very critical for obtaining optimum performance from components/devices. X-ray diffraction (XRD) is an accurate, reliable, non-destructive and repeatable method to investigate residual stress levels through precise characterization of interplanar lattice spacing in engineering components (Warren, 1969; Cullity, 1978; Noyan & Cohen, 1987; Oshioka, 1993). The unique non-destructive nature of this measurement technique is especially advantageous in the context of engineering applications, since it allows the evaluation of stresses and microstructural parameters of real structural components without material removal.

Synchrotrons provide very intense beams of high-energy X-rays, and therefore have a much higher depth of penetration as compared with conventional sources. Also, wavelength tunability provides the possibility of carrying out depth-resolved stress measurements desired by industry and academics. Due to good collimation of the source, synchrotron

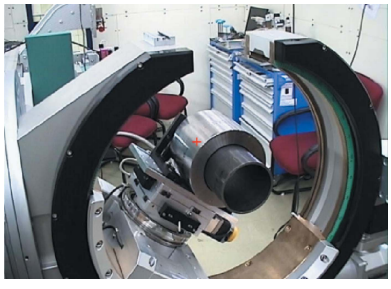

X-ray diffraction is capable of providing high spatial resolution (~500 mm). Thus, 3D mapping of the strain distribution in engineered components up to millimetre depths (Steuwer *et al.*, 2004; Korsunsky *et al.*, 2006; Pyzalla, 2000; Collins *et al.*, 2017) is possible.

Although synchrotron-based XRD is a very useful tool for measuring residual stresses in a variety of samples/components, beamline facilities having dedicated setups for stress measurements on large components/samples are very scarce which limits their practical application (Guo *et al.*, 2021). In view of this, and considering numerous advantages of the synchrotron XRD technique, a multipurpose X-ray scattering beamline has been recently commissioned at the bending-magnet port of the third-generation synchrotron source Indus-2 (2.5 GeV, 300 mA), India. This beamline is a national facility fully funded by the Department of Atomic Energy (DAE), Government of India, for its construction and operation. The beamline can operate in various beam modes: monochromatic focused beam, monochromatic parallel beam, pink and white beam modes. The flexible beamline design allows switching between different operational modes within a short time (~30 minutes) and thus enables a wide range of X-ray scattering experiments such as stress measurement, texture analysis, phase identification, microstructure determination, kinetic studies, anomalous scattering, grazing-incidence XRD (GIXRD), high-resolution XRD, X-ray reflectivity (XRR) and energy-dispersive XRD (EDXRD).

One of the thrust areas of interest of this beamline is to carry out residual stress measurements in thin films and bulk materials. This beamline has an open Eulerian cradle six-circle diffractometer which allows stress measurement at high 2θ values in both iso- and side-inclination modes. Another distinct feature of the beamline is the capability to handle large size samples up to ~1000 mm length, ~500 mm width and ~45 mm thickness with maximum sample weight up to ~12 kg. This feature makes it suitable for carrying out stress measurement on actual or prototype engineering components. This beamline also has provision for testing large size synchrotron optics in the 5–25 keV energy range.

Additionally, this beamline will incorporate the facility of *in situ* XRD during mechanical deformation. The observed behavior under *in situ* conditions would provide useful input for developing computational simulation tools for engineers to predict the performance of materials and components. Also, *in situ* characterization of materials under non-ambient conditions will help gain a deeper understanding of the microstructure–physical properties correlation (Miller *et al.*, 2020). These facilities will be useful in developing efficient engineering components required for industries, *e.g.* nuclear and aerospace.

The present article reports on the construction and commissioning of a versatile X-ray scattering and diffraction beamline for engineering applications (BL-02) at a bending-magnet port of the Indus-2 synchrotron source, India. A few initial results are also presented to demonstrate the capabilities of the beamline. Future upgrades planned for the beamline are also briefed.

Table 1
Summary of the design specifications for the engineering applications beamline.

Characteristic	Specification
Source	Bending magnet
Energy range	
Monochromatic beam mode	5–25 keV
Pink beam mode	5–25 keV
White beam mode	5–45 keV
Collimating and focusing mirrors	1.2 m-long Pt-coated Si mirrors
Incidence angle	3 mrad
Double-crystal monochromator	Si (111) flat crystal pair 25 mm crystal offset
Length of the beamline	~39 m from the tangent point
Beam acceptance	2 mrad (H) × 0.2 mrad (V)
Flux on the sample	
Monochromatic beam mode (spectral flux)	$\sim 10^{11}$ photons s^{-1} (0.1% bandwidth)$^{-1}$ at 10 keV
Pink beam mode (total flux)	$\sim 10^{14}$ photons s^{-1}
White beam mode (total flux)	$\sim 10^{15}$ photons s^{-1}
Beam size at the sample	
White beam mode	0.5–1 mm (H) × 0.5–1 mm (V)†
Monochromatic focused beam mode	0.36 mm (H) × 0.39 mm (V)
Monochromatic parallel beam mode	8 mm (H) × 0.75 mm (V) (maximum)†
Pink beam mode	0.37 mm (H) × 0.39 mm (V)
Energy resolution ($\Delta E/E$)	1.5 $\times 10^{-4}$ at 10 keV

† Controlled by slits.

2. Beamline overview

This section describes the source, optical design and installed components at the engineering applications beamline. A summary of all the operation modes is presented with the beamline optics used for each mode. Finally, details about the endstations are given where XRD experiments are performed.

2.1. Source

Indus-2 is a third-generation Indian synchrotron radiation (SR) source, designed for 2.5 GeV beam energy and 300 mA ring current (Singh *et al.*, 2006; Deb *et al.*, 2013). The engineering applications beamline (BL-02) is installed on a 10° port of a first bending magnet (DP-1) of the double-bend acromat lattice at Indus-2 (Sahni *et al.*, 2009; Singh *et al.*, 2006). The r.m.s. electron source size at the center of the bending magnet is 257 μm (H) × 232 μm (V) and the estimated photon source size (FWHM) is ~600 μm (H) × 500 μm (V). Indus-2 is currently operating at 2.5 GeV beam energy and 200 mA beam current.

2.2. Beamline optics

The engineering applications beamline is configured to operate in white beam, pink beam and monochromatic beam modes. The flexible optical design of the beamline enables easy switching between different operational modes. A summary of the beamline design parameters in different beam operating modes is presented in Table 1.

The beamline consists of a front-end (Raghuvanshi *et al.*, 2007), optics hutch, two experimental hutches and a control station. The optical layout of the beamline showing the major components and their distances from the tangent point is

illustrated in Fig. 1. The beamline optics comprised a collimating mirror (M1), a Si(111) double-crystal monochromator (DCM) and a toroidal mirror (M2) with sagittal and vertical focusing capability. Various X-ray beam diagnostic elements such as slits are also in place to diagnose and define the beam (Fig. 1).

A 200 µm beryllium (Be) window bonded to a water-cooled copper body placed at a distance of ∼16 m from the tangent point separates the front-end of the beamline from the other optical elements. The average heat load of the synchrotron beam is ∼30 W mrad^{-1} (H); as the horizontal acceptance of the beamline is 2 mrad, this becomes ∼60 W at the first Be window. Most of the heat load is taken away by this water-cooled Be window, which transmits radiation above ∼2 keV. In order to protect the subsequent beamline components from the heat load, all the beamline components up to the exit Be window are water-cooled.

Just after the beryllium window, a water-cooled diagnostic system (S1) is installed which has a four-blade slit, a beam viewer (phosphor screen Eu-doped gadolinium oxysulfide, P43) and tungsten wire monitor to define the beam size and also to measure the beam profile. The four-blade slit has two pairs of tungsten blades for shaping the beam as per the requirement. The beam profile is obtained with the beam position monitor by measuring the photo-electron current by scanning the wire across the beam with a step size as small as 0.1 mm.

To vertically collimate the beam, a water-cooled mirror (pre-mirror, M1) having meridional cylinder shape is used. The mirror is 1.2 m long and 80 mm wide, having a 300 Å Pt coating on a single-crystal Si substrate. The pre-mirror is located at ∼17.2 m from the source and is deflecting the SR beam down. The meridional radius of curvature for M1 could be varied from ideal flat to 11.50 km with the help of a cylindrical bender. M1 is used to collimate the beam in the meridional plane and also acts as a low energy pass filter up to 25 keV.

After the pre-mirror, a water-cooled diagnostic system (S2), similar to S1, is installed to detect the beam position and profile of the beam after reflection from M1.

To monochromatize the synchrotron beam at the required energy between 5 and 25 keV, a Si(111) double-crystal monochromator having a crystal pair with (+,−) geometry (Shvyd'ko, 2004) with the Bragg reflection in the upward direction from the first flat crystal is placed at ∼21.2 m from the source. It is equipped with a cooling system to prevent deformation of crystals from the heat load. The footprint of the beam on the crystal increases with increasing energy because of smaller incidence angles at higher energies. Thus, the dimensions of both the crystals were decided so as to accept the full beam at 25 keV energy; the first crystal with an optical area of 70 mm (width) ×70 mm (length) and thickness of 10 mm and the second crystal with an optical area of 65 mm (width) × 200 mm (length) and thickness of 15 mm were used. The first crystal monochromatizes the beam whereas the second crystal provides monochromatic X-ray beam at fixed exit parallel to the incident beam with a beam offset of 25 mm.

To focus the beam in both the horizontal and vertical plane at the experimental station, a 1.2 m-long and 80 mm-wide Pt-coated post-mirror (M2) in the form of a toroidal shape is used. For the toroidal mirror, the meridional and sagittal radii of curvature are 5.405 km and 47.36 mm, respectively. This mirror is fitted to a cylindrical bender, which manipulates the mirror meridional radii over the range from ideal flat to 5.4 km; however, the sagittal radius of curvature is fixed. M2 is used with a 2:1 demagnification to minimize aberrations such as astigmatism and coma (Peatman, 1997).

The beamline design incorporates a flexible operation where experiments can be carried out in various configurations of optical elements, *i.e.* M1, M2 and DCM. In order to achieve this, the optics layout has been designed in such a way that the beam height variations at the experimental station placed 35.4 m away from the source is within 90 mm from white beam mode (top position) to monochromatic parallel beam mode (bottom position). To achieve this objective, the M1 mirror is used in a bounce-down configuration, followed by the DCM whose crystals bump the beam up by 25 mm, and finally a bounce-up M2 mirror. To operate the beamline in various configurations, the combinations of DCM and mirrors used is as per the following scheme:

(i) Use of both mirrors (M1 and M2) and DCM (monochromatic focused beam mode).

(ii) With only the M1 and DCM in place (monochromatic parallel beam mode, in the vertical plane only), using this

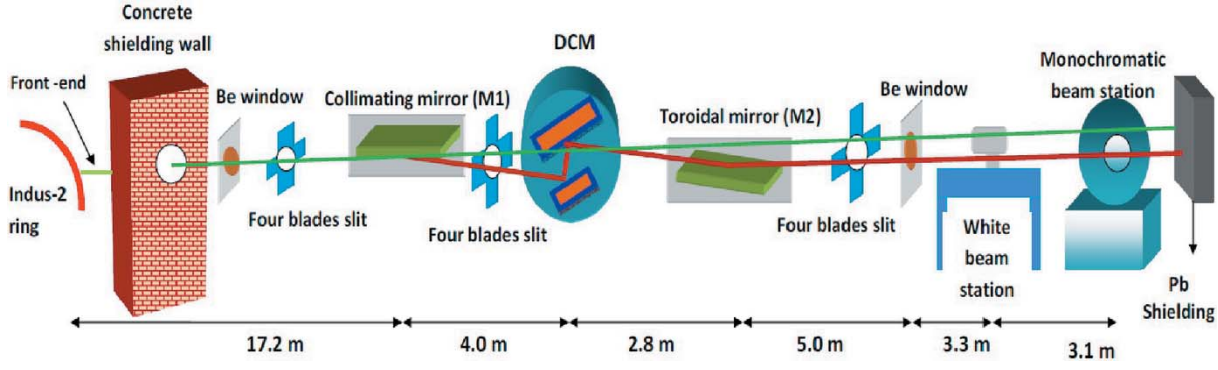

Figure 1
Schematic layout of the engineering applications beamline at Indus-2 (not to the scale).

configuration a beam with 2 mrad horizontal divergence is obtained.

(iii) With M1 and M2 mirrors only (pink beam mode: focused or parallel).

In pink beam mode, a band of energy is selected using both the mirrors (M1 and M2). M1 is kept at a fixed incidence angle of ∼3 mrad and, by changing the incidence angle of the post-mirror (M2) (between 3 mrad and 3.66 mrad), the range of the energy bandpass, *e.g.* 5–25 keV or 5–20 keV, can be selected, as the mirror would only reflect energies below a certain threshold. The incidence angle of M2 can be changed in a limited range only because changing the incidence angles also causes a shift in the beam direction. In addition, X-ray absorbing foils can be placed in the beam path to remove low-energy X-rays. Thus, a tunable broad bandwidth, with an X-ray flux that is more than ∼1000 times that of a monochromatic beam, would be achieved using the pink beam. The pink beam can be used as a parallel beam or a focused beam.

(iv) Without either mirror and DCM (white beam mode). The available energy range for white beam mode is 5 to 45 keV, whereas for both the monochromatic and pink beam modes the available energy range is 5 to 25 keV.

The beamline is divided into seven vacuum sections through the use of beryllium windows and gate valves. The exit beryllium window is protected from ozone using a helium-filled chamber. The beamline optics is enclosed in the first hutch and the endstations are located in separate experimental hutches subsequently. Details of the endstations are described in the next section.

2.3. Endstations

The engineering applications beamline simultaneously hosts two experimental stations – the white beam station and the monochromatic beam station – along the beam path. These stations can be used alternately as per requirement. The first station is located at a distance of 32.3 m and the second station is at 35.4 m from the bending-magnet source.

The first endstation is employed primarily for investigations of strain scanning and fast phase detection by EDXRD experiments. It is designed for carrying out dynamic studies on the samples as a full diffraction pattern can be recorded in a very short time without any sample movement. This station can also be very useful for studying thin films during growth or analyzing heat-induced phase transformations in samples. With the white SR beam from the bending magnet having a reasonable intensity up to 45 keV and a wide range of 2θ angle selectivity of $\pm 25^{\circ}$, one can record the diffraction data up to a q range of ~ 15 Å^{-1} at this endstation. Diffracted X-rays from the sample can be energy analyzed using either a Peltier-cooled vortex AMETEK silicon drift detector (SDD) or a liquid-nitrogen-cooled high-purity germanium (HPGe) detector. It is a versatile station that can be customized to accommodate the samples of various shapes and sizes as per the user requirement. The pink beam will also be brought to this endstation for testing in-house-developed optics and detectors *etc.*, where a source of limited bandwidth would be required.

The second experimental station houses a high-precision open Eulerian cradle six-circle Huber diffractometer supporting two detectors (described at the end of this section). This endstation can accommodate a sample up to ∼12 kg in weight and has a sphere of confusion of 50 µm for all axis movement. It can handle a sample size up to ∼1000 mm length, ∼500 mm width and ∼45 mm thickness. The open Eulerian cradle of this diffractometer allows a high 2θ range up to 170° with a step size accuracy of 0.0002°. High-temperature stages are available for *in situ* XRD studies up to 600°C in a controlled atmosphere, *i.e.* high vacuum or inert gas. As per the user requirement, other customized setups for sample stages and environmental cells can also be adapted. This station is equipped with a large-area 2D detector (Dectris Pilatus 3X100 K-A 1000 µm HPC detector) and position-sensitive Mythen detector (MYTHEN2 X 1K) for rapid measurements. The diffractometer is controlled through *SPEC* software (see http://www.certif.com) for data acquisition. This endstation will be utilized for structural investigations and strain/stress and texture determination on bulk samples as well as on thin films. Two beam configurations, *viz.* monochromatic focused beam mode and monochromatic parallel beam mode, will be used at this endstation for performing experiments such as powder diffraction, GIXRD, XRR, anomalous scattering *etc*. Monochromatic parallel beam mode would be important for experiments requiring ultra-high-angular resolution, but, for cases where moderate resolutions would be sufficient, monochromatic focused beam mode would be preferred to gain the advantage of high flux and to minimize the data acquisition time.

3. Performance of the beamline

The present section describes the beamline performance wherein various beam parameters – beam size, flux, resolving power *etc.* – were determined, and a few initial results are presented. All the measurements were performed in monochromatic parallel beam mode, *i.e.* using only M1 and DCM. In the case of EDXRD measurement, M1 and DCM are also retracted from the beam path to obtain white beam.

3.1. Beam characterizations

The beamline flux was measured as a function of photon energy at ∼36 m from the X-ray source (*i.e.* at the monochromatic experimental station). A calibrated photodiode was used to measure the beamline flux at the available energy range in the monochromatic parallel beam mode. The maximum total photon flux was measured as $\sim 1.12 \times 10^9$ photons s^{-1} at the X-ray beam energy of ∼12 keV. Photon flux was measured using a calibrated AXUV100 photodiode placed close to the sample position. The slit opening was kept as 5 mm (H) × 0.2 mm (V). The storage ring current used for the flux calculation was 100 mA.

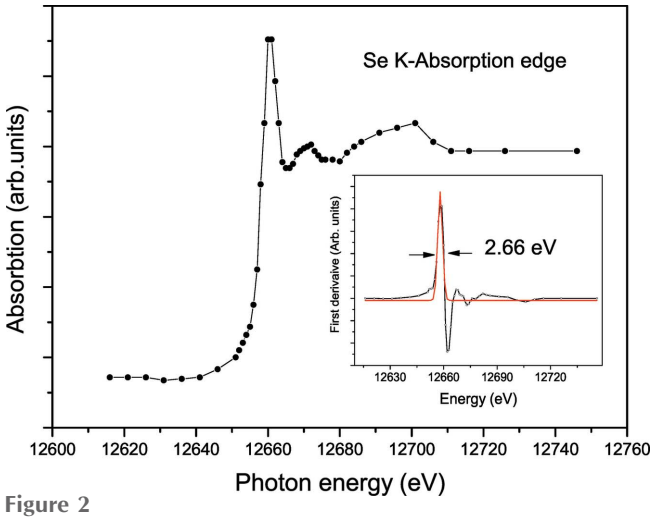

Figure 2
X-ray absorption data near the Se *K*-edge measured at the beamline. The inset shows the first derivative of the data.

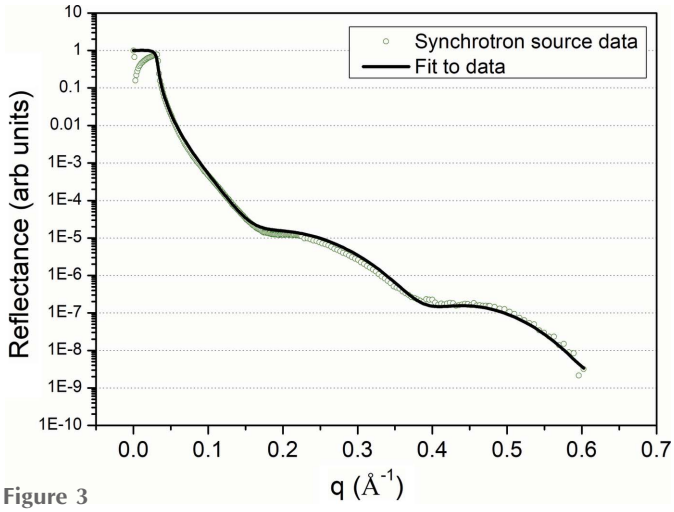

Figure 3
X-ray reflectivity (XRR) measurements on polished float glass substrate carried out at the engineering applications beamline (BL-02).

The theoretical energy resolution from a Si(111) DCM is $\sim 1.4 \times 10^{-4}$, appopriate for XRD experiments and for *K*-edge XAS experiments in most transition metals. In order to demonstrate this, an X-ray absorption spectroscopy (XAS) measurement was performed at the Se *K*-edge (12658 eV), which has an intrinsic orbital broadening (~2.33 eV) larger than the instrumental resolution. The XAS measurement was performed in transmission mode using an Se standard foil (40 µm) procured from Exafs Materials, USA. The absorption data near the Se *K*-edge is shown in Fig. 2; the inset gives the first derivative of the absorption data. It can be seen clearly that the intrinsic value (~2.66 eV) is almost obtained. This shows that the resolution achieved using the Si(111) DCM is close to the theoretical value and that the use of a Si(111) DCM is adequate for the beamline purposes.

3.2. X-ray reflectivity measurements

XRR is a very important tool for determining thin film thickness, roughness and density of layers. To obtain a high dynamic range and repeatable XRR data a fine parallel beam should pass through the center of rotation of the ω circle of the goniometer and a series of aligned slits must be placed before the sample and detector to reduce the background signal. Repeatable XRR measurements are confirmation of the correct alignment of the goniometer.

XRR measurement was performed on a polished float glass substrate using a beam energy of 15 keV and beam size of ~6 mm (H) × 0.05 mm (V). The goniometer was aligned with respect to the beam such that the ω axis is within ±0.02 mm of the beam center. Measurements were performed using a Huber goniometer with step size of 0.005° for ω/θ movement and 0.01° for 2θ movement. A MYTHEN2 X 1K detector was used in point scan mode for the measurement. Fig. 3 shows the XRR measurements performed on a polished float glass substrate at the beamline. XRR data were successfully measured with more than eight orders of dynamic range and a q range up to ~0.6 Å^{-1} was recorded. The measured data were simulated using *Parratt 32* software (Parratt, 1954) and the best fit to the data was obtained considering a low-density top layer on the polished float glass substrate. The substrate roughness was obtained as ~3.1 ± 0.5 Å, whereas the low-density top layer has a thickness and roughness of 27.0 ± 0.5 Å and ~3.2 ± 0.5 Å, respectively. Thus, the broad oscillations in SR XRR data of the float glass substrate may be ascribed to the presence of a low-density layer on top of the substrate. This top layer is formed due to porosity becoming induced during polishing of the float glass substrate. Further, it may be noted that the availability of a high dynamic as well as a q range in the SR-XRR data is useful to obtain the correct estimation of roughness and thickness in the case of such low thickness layers/films.

3.3. Angle-dispersive X-ray diffraction (ADXRD) measurement

The X-ray diffraction pattern of NIST SRM 660C LaB_6 standard sample was measured in monochromatic parallel beam mode of the beamline (where only M1 and DCM were used to obtain a parallel beam). The incident beam size was defined as ~6 mm (H) × 0.12 mm (V) with the help of slits in the incident beam path. XRD measurement was carried out in θ–2θ reflection geometry using a Huber diffractometer equipped with a MYTHEN2 X 1K position-sensitive strip detector (PSD). The PSD was placed at a distance of ~1065 mm from goniometer center covering a total 2θ range of ~3.435°. The PSD has a total of 1280 pixels, with one pixel corresponding to ~0.002683°. The beam energy of ~12 keV (~1.037 Å) was used for the measurement. The XRD pattern was recorded in a 2θ range of 10° to 115°. An SRM powder sample was filled into a glass sample holder of diameter 15 mm and thickness ~0.15 mm and rotated at ~45 r.p.m. during measurements. The data were collected at 20 s per frame.

Fig. 4 shows a powder diffraction pattern recorded for the standard sample at the engineering applications beamline (BL-02). *FullProf* software (Rodríguez-Carvajal, 1993) was

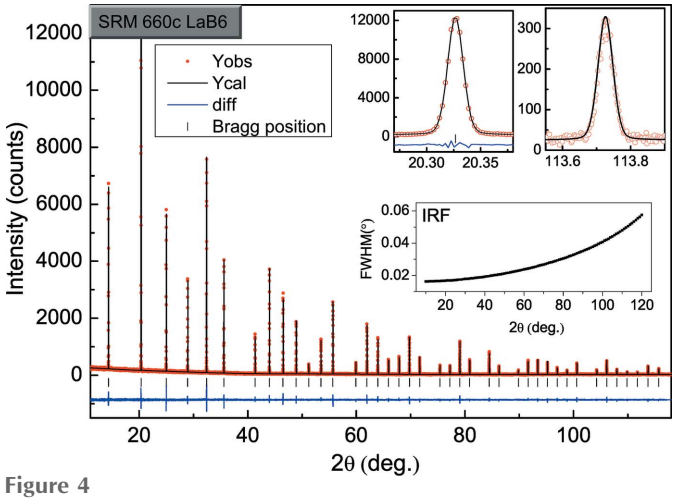

Figure 4
The Le Bail fitting of NIST SRM 660C LaB_6 powder pattern measured at 12 keV: experimental data (red circles) and fitted (blue line), with their difference (residual, line below). Insets show fitting profiles of low- and high-angle peaks and IRF. *R*-factors of refinement are: R_p, 8.51%; R_{wp}, 11.7%; R_{exp}, 11.04%; χ^2: 1.12.

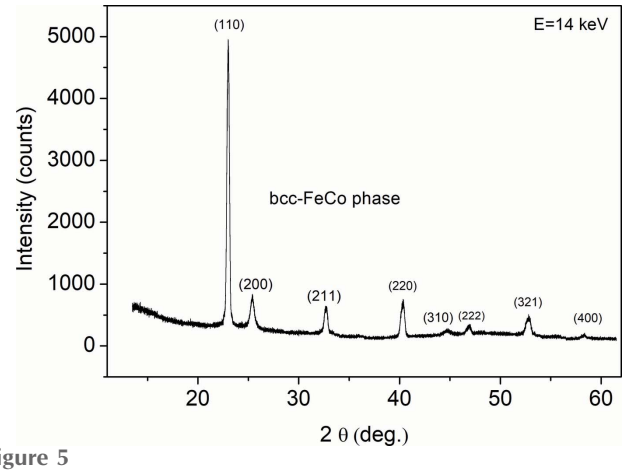

Figure 5
GIXRD data of metallic alloy thin film taken using a beam energy of 14 keV.

used for the Le Bail fitting (Le Bail *et al.*, 1988) of synchrotron powder XRD data and the resultant fitting is also included in the same figure. The peak profiles were described using a pseudo-Voigt function, and Caglioti's equation (Caglioti *et al.*, 1958) was used for estimation of the full width at half-maximum (FWHM) with scattering angle. The insets of Fig. 4 show the fitting quality of low- and high-angle peaks and the corresponding instrument resolution function (IRF) derived from fitting. During refinement, the lattice parameters were kept fixed as per the certified value of SRM 660C. The observed FWHM was found to be ∼0.016° at 18° and ∼0.05° at 113° of the 2θ angle, and the Lorentzian fraction was found to be ∼0.19–0.25 in this 2θ range. The widths of the Bragg peaks of an XRD pattern have contributions from both the instrument and the sample-related broadening. Instrument resolution plays a vital role in the structural and microstructural analysis of a sample. The high resolution achieved with standard powder would be helpful to generate high-quality data for obtaining detailed and reliable microstructural details using the line profile (Rebuffi *et al.*, 2014). Recently, this beamline was used to study the microstructure of iron powder using line profile analysis. The super-Lorentzian peak shape of single-phase Fe powder was ascribed to two microstructures having different microstrains (Bhakar *et al.*, 2021).

GIXRD measurement at the synchrotron source has its own advantages due to the salient properties of synchrotron X-rays. One of them is the small size of the synchrotron X-ray source, which allows GIXRD measurements to be performed in a small area on the sample. Also, the intensity of synchrotron X-rays is much higher than for a conventional X-ray source and thus the data collection time is much shorter when using synchrotron X-rays.

Fig. 5 shows GIXRD measurements performed on 50 nm FeCoNbB alloy thin film coated on Si(100) substrate. The beam energy of ∼14 keV was used for the measurement. The angle of incidence was kept fixed as 0.6° and the beam size was defined as ∼5 mm (H) × 100 µm (V) using the incident slit. The full diffraction pattern was recorded in 20 minutes using the MYTHEN2 X 1K detector in line scan mode.

3.4. Residual stress measurement

This beamline is primarily designed to carry out residual stress measurement from thin films to large size bulk samples or on components. The most commonly used method for stress measurement is the $\sin^2\Psi$ technique (Noyan & Cohen, 1987). In this method the interplanar spacing (*d*) of a selected (*hkl*) plane is determined at multiple inclination angles (Ψ) from the sample surface normal. In regular *d* versus $\sin^2\Psi$ measurements one needs to attain a high value of Ψ for obtaining correct and reproducible stress measurements. The inclination of the sample can be done in both iso-inclination and side-inclination (χ rotation) methods. In the iso-inclination method, to obtain high Ψ measurement it is essential to select a diffraction peak at the highest possible 2θ value. At high 2θ values the intensity of the diffraction peak becomes very low, thus a longer measurement time is required for obtaining a good signal-to-noise ratio. On the other hand, in the side-inclination method one can obtain high Ψ measurement even with low 2θ diffraction peaks, hence a much better signal-to-noise ratio can be obtained in a short measurement time. In addition to this, the side-inclination method is preferred over the iso-inclination method as absorption corrections due to the path difference in the incident and diffracted beam at different Ψ are not required (Noyan & Cohen, 1987). In this article the stress measurements were performed using the side-inclination method.

Stress measurements were performed using the six-circle diffractometer having an open χ circle with a travel range of −60° to 90°. In the side-inclination method, alignment of the sample height and beam position at the rotation axis of the goniometer is very critical. Thus, a fine beam of 250 µm (H) × 150 µm (V) was selected with the help of incident beam cross slits so as to avoid the beam size variation with Ψ. The selected fine beam was aligned such that it should pass through the

rotation axis of the goniometer within the sphere of confusion for compound motion of all four axes, *i.e.* within 50 µm accuracy.

For such precise alignment the four-axis goniometer is mounted on an *XZ* stage which can move horizontally by ±30 mm and vertically by ±50 mm with 10 µm accuracy. The alignment of the X-ray beam passing through the center of the rotation axis of the goniometer was ensured with the help of X-ray sensitive film (XR-QA2 film), and no movement in X-ray beam spot position with changing Ψ was recorded. Correctness of alignment was further confirmed by carrying out *d* versus $\sin^2(\Psi)$ measurement on a stress-free standard powder where no slope in the *d* versus $\sin^2(\Psi)$ plot was observed. Fig. 6(*a*) shows a *d* versus $\sin^2(\Psi)$ plot for corundum (Al_2O_3) powder for two different diffraction planes (1 1 10) and (1 1 9) measured using a beam energy of 15 keV. These measurements yielded an almost flat *d* versus $\sin^2(\Psi)$ curve indicating that stress is zero in the powder [Fig. 6(*a*)], and also confirms that alignment of the goniometer is correct. Further, the stress measurement was carried out on the Ti standard samples provided by PRTO XRD, Canada. The sample has a locked-in stress of 760 ± 35 MPa measured for (213) *hkl* using Cu *Kα* (8.047 keV energy). Stress measurement was performed on this sample for the (110) plane using 15 keV beam energy. To check the repeatability, about 20 repeat measurements were made using the method described above. Measured stress values are varying from 690 to 740 MPa. This

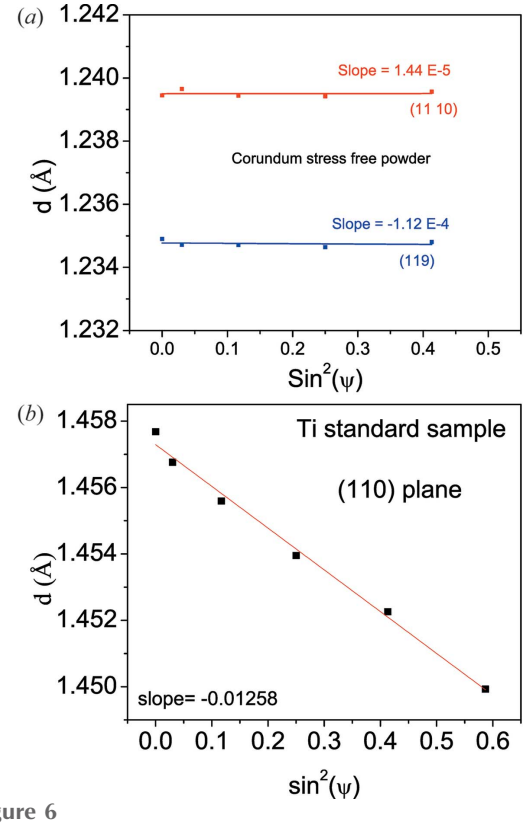

Figure 6
(*a*) Plot of the *d* versus $\sin^2(\Psi)$ curve for (*a*) stress-free corundum (Al_2O_3) powder. (*b*) Stresses of the Ti standard sample. Stress measurements were made in side-inclination mode using a beam energy of 15 keV.

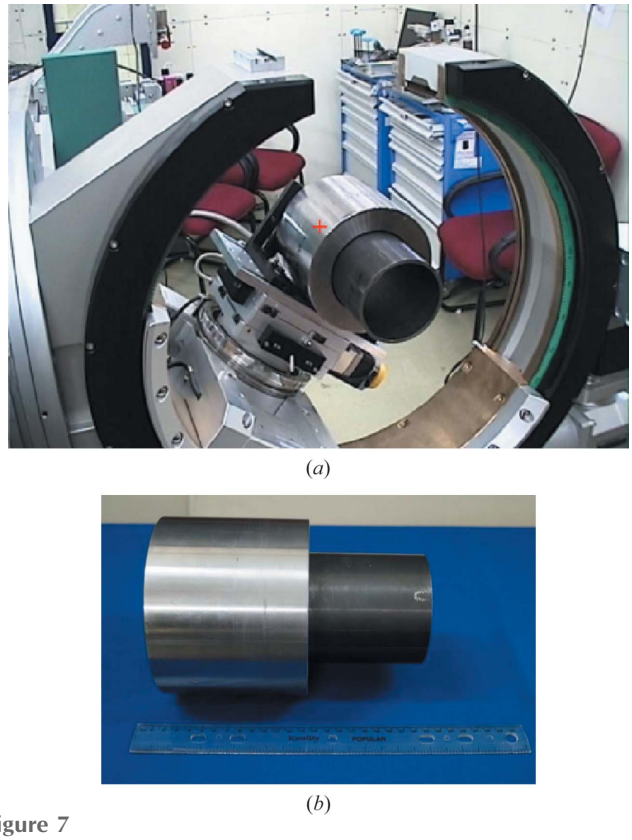

Figure 7
(*a*) Photograph of the welded tube loaded on the monochromatic experimental station. (*b*) Photograph of the weld joint showing dimensions.

indicates a mean stress value of 715 ± 25 MPa. Fig. 6(*b*) shows a representative *d* versus $\sin^2(\Psi)$ curve for the pre-stressed Ti sample for the (110) plane. The observed lower spread and difference in the measured stress value may be ascribed to the use of shorter wavelength and a different (*hkl*) plane in the present case.

To demonstrate the capability of handling large size samples/components, residual stress measurement was performed on a zircaloy to SS tube weld weighing ∼11 kg, of length ∼200 mm and diameter ∼140 mm, at the monochromatic endstation of the beamline. Fig. 7 shows the sample mounted on the goniometer for the measurement. Details of the measurement will be published elsewhere.

3.5. Energy-dispersive X-ray diffraction (EDXRD) measurement

For EDXRD measurement, the beamline was operated in white beam mode, which accepts the full white synchrotron beam ranging from 5 to 45 keV. Fig. 8 shows representative EDXRD measurements carried out at the white beam experimental station on NIST SRM 660B LaB_6 standard powder using the two-circle goniometer. Data were collected using the Peltier-cooled SDD kept at a fixed angle of $2\theta \simeq 12^\circ$ in reflection geometry. The data collection time was 50 s. *FullProf* software (Rodríguez-Carvajal, 1993) was used for the Le Bail fitting of the synchrotron powder EDXRD data of

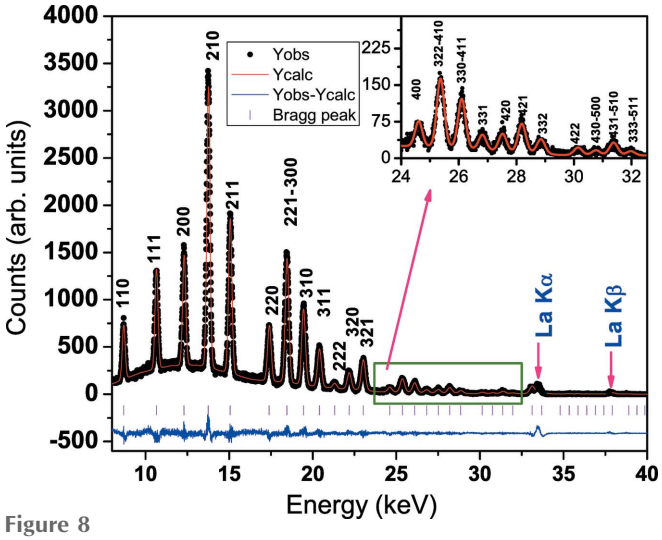

Figure 8
The Le Bail refinement fitting of NIST SRM 660B. The inset shows low-intensity peaks at high energy. Here, black circles represent the synchrotron powder EDXRD data, and red and blue lines represent the fitted curve and difference curve, respectively.

LaB_6 by keeping the lattice parameters fixed at standard values. Stress measurements were also performed using the EDXRD setup and it was observed that, due to the poor energy resolution of the detector (1.2%) in the available energy range (up to 40 keV), it was not possible to reliably resolve stress values lower than 250 MPa. Integration of the liquid-nitrogen-cooled HPGe detector was also performed for recording EDXRD data up to the high energy range (∼45 keV).

The observed energy resolution of this detector is ∼0.5% at 40 keV which is better than that of the Peltier-cooled Si (Li) detector. But it is observed that, for the quantification of stresses below 250 MPa, a high-energy incident beam (more than 60 keV) would be required. However, the present set-up is promising for dynamic studies and for scanning of samples for assessment of stress concentration zones in large samples.

4. Conclusions

An X-ray scattering and diffraction-based beamline for engineering applications has been installed at the bending-magnet port of the Indian synchrotron source, Indus-2. It has a working energy range of 5–45 keV in white beam mode and 5–25 keV in monochromatic beam mode. The detailed design, layout, operation modes and measurement capabilities of the beamline have been described herein. The flexible design of the beamline allows easy switching between various operation modes and thus facilitates a wide range of experiments. The versatility of the beamline has been demonstrated by performing a variety of experiments such as powder XRD, XRR, GIXRD, EDXRD and residual stress measurements *etc*. The capability of accommodating large size has been demonstrated by carrying out stress measurements on a 11 kg, 200 mm-diameter tube weld. Also, the high resolution of the beamline has been used to study the microstructure of iron powder using line profile analysis. This beamline will be useful in generating inputs for simulation tools to predict and confirm the performance of materials. In the future, it is planned to integrate an *in situ* loading system for estimating the X-ray elastic constant of different materials and alloys, a large-area 2D detector system for dynamic studies on thin films and bulk samples, and low-temperature and high-temperature heating stages to enhance beamline facilities for a range of experiments.

Acknowledgements

The authors are thankful to Shri Debashish Das, Director, RRCAT, Shri S. V. Nakhe, Director, MSG, and Dr Tapas Ganguli, Head SUS, for the support extended by them throughout the installation and commissioning of the beamline. The authors are also thankful to alignment team, RRCAT, for providing help in the alignment of some of the critical components of the beamline. The authors are also thankful to Dr Dileep Kumar, UGC-DAE-CSR, for providing help in the EDXRD set-up. The members of the mechanical and electronics group, SUS, are also acknowledged for their help in installation of various components of the beamline. The authors are also thankful to Dr P. A. Naik, Ex-director, RRCAT, for his constant encouragement and help.

References

Bhakar, A., Gupta, P., Rao, P. N., Swami, M. K., Tiwari, P., Ganguli, T. & Rai, S. K. (2021). *J. Appl. Cryst.* **54**, 498–512.
Caglioti, G., Paoletti, A. & Ricci, F. P. (1958). *Nucl. Instrum.* **3**, 223–228.
Collins, D. M., Erinosho, T., Dunne, F. P. E., Todd, R. I., Connolley, T., Mostafavi, M., Kupfer, H. & Wilkinson, A. J. (2017). *Acta Mater.* **124**, 290–304.
Cullity, B. D. (1978). *Elements of X-ray Diffraction.* Reading: Addison-Wesley.
Deb, S. K., Singh, G. & Gupta, P. D. (2013). *J. Phys. Conf. Ser.* **425**, 072009.
Guo, J., Fu, H., Pan, B. & Kang, R. (2021). *Chin. J. Aeronaut.* **34**, 54–78.
Korsunsky, A. M., Liu, J., Golshan, M., Dini, D., Zhang, S. Y. & Vorster, W. J. (2006). *Exp. Mech.* **46**, 519–529.
Le Bail, A., Duroy, H. & Fourquet, J. L. (1988). *Mater. Res. Bull.* **23**, 447–452.
Miller, M. P., Pagan, D. C., Beaudoin, A. J., Nygren, K. E. & Shadle, D. J. (2020). *Metall. Mater. Trans. A*, **51**, 4360–4376.
Noyan, I. C. & Cohen, J. B. (1987). *Residual Stress Measurement by Diffraction and Interpretation.* New York: Springer-Verlag.
Oshioka, Y. (1993). *X-ray Diffraction Studies on the Deformation and Fracture of Solids*, edited by K. Tanaka, S. Kodama & T. Goto, pp. 109–134. Cambridge University Press.
Parratt, L. G. (1954). *Phys. Rev.* **95**, 359–369.
Peatman, W. B. (1997). *Gratings, Mirrors and Slits.* Amsterdam: Gordon Science.
Pyzalla, A. (2000). *J. Non-Destruct. Eval.* **19**, 21–31.
Raghuvanshi, V. K., Dhamgaye, V. P., Singh, A. K. & Nandedkar, R. V. (2007). *AIP Conf. Proc.* **879**, 631–634.
Rebuffi, L., Plaisier, J. R., Abdellatief, M., Lausi, A. & Scardi, P. (2014). *Z. Anorg. Allg. Chem.* **640**, 3100–3106.
Rodríguez-Carvajal, J. (1993). *Physica B*, **192**, 55–69.
Sahni, V. C., Chia, S., Ratnavelu, K. & Muhamad, M. R. (2009). *AIP Conf. Proc.* **1105**, 180–187.

Shvyd'ko, Y. (2004). *X-ray Optics*, Vol. 98 of *X-ray Optics. Springer Series in Optical Sciences.* Berlin, Heidelberg: Springer.
Singh, G., Abdurahim Banerji, A., Barpande, K., Bhatnagar, V., Bhujle, A. G., Fakhri, A. A., Fatnani, P., Ghodke, A. D., Hannurkar, P. R., Holikatti, A. C., Husain, R., Jena, S. K., Kant, P., Kotaiah, S., Kumar Pradeep Lad, M., Marathe, R. G., Pravinkumar, M., Puntambekar, T. A., Sahni, V. C., Saini, R. S., Sharma, A., Shridhar, R., Shukla, S. K., Thakurta, A. C., Thipsay, A. P., Tiwari, S. R., Thakur, D. S. & Vats, D. K. (2006). *Proceedings of the 3rd Indian Particle Accelerator Conference (InPAC-2006)*, 1–4 November 2006, Mumbai, India, pp. 94–97.
Steuwer, A., Santisteban, J. R., Turski, M., Withers, P. J. & Buslaps, T. (2004). *J. Appl. Cryst.* **37**, 883–889.
Warren, B. E. (1969). *X-ray Diffraction*. New York: Addison-Wesley.